Plant Physiol. (1992) 100, 614-619
0032-0889/92/100/0614/06/$01.00/0

Received for publication February 21, 1992
Accepted May 4, 1992

Electric Current Precedes Emergence of a Lateral Root in Higher Plants

Shingo Hamada, Shu Ezaki, Kenshi Hayashi, Kiyoshi Toko*, and Kaoru Yamafuji

Department of Electronics, Faculty of Engineering, Kyushu University 36, Fukuoka 812, Japan (S.H., K.H., K.T., K.Y.); and Department of Electric Engineering, Faculty of Engineering, Kinki University in Kyushu, Iizuka 820, Japan (S.E.)

ABSTRACT

Stable electrochemical patterns appear spontaneously around roots of higher plants and are closely related to growth. An electric potential pattern accompanied by lateral root emergence was measured along the surface of the primary root of adzuki bean (*Phaseolus angularis*) over 21 h using a microelectrode manipulated by a newly developed apparatus. The electric potential became lower at the point where a lateral root emerged. This change preceded the emergence of the lateral root by about 10 h. A theory is presented for calculating two-dimensional patterns of electric potential and electric current density around the primary root (and a lateral root) using only data on the one-dimensional electric potential measured near the surface of the primary root. The development of the lateral root inside the primary root is associated with the influx of electric current of about 0.7 $\mu A \cdot cm^{-2}$ at the surface.

The electrochemical field surrounding and within living bodies is suggested to be important for growth or development (10, 12). Plant roots make stable electrochemical patterns around themselves spontaneously (1, 6, 11, 22, 25, 26). These patterns are closely related to growth, and hence the elongation of roots and shoots can be controlled by an electric field and voltage applied externally (7, 9, 15) and disturbance of such patterns causes suppression of elongation (24). Similar electrochemical patterns are observed in unicellular systems (2, 4, 5, 25) and the electric asymmetry also appears in gravireception (20).

In this paper, an electric potential pattern preceding lateral root emergence was measured along the surface of a primary root by the microelectrode technique. The electric potential became lower at the emerging point, preceding the emergence of a lateral root by about 10 h. We also provide a theory for calculating two-dimensional patterns of electric potential and electric current density around the primary root using only the measured electric potential near the surface of the primary root. This theory is consistent with the observed two-dimensional pattern of electric potential previously reported (8). Thus, the two-dimensional pattern of electric current can be calculated for any stage of lateral root emergence. The development of the lateral root inside the primary root is associated with an electric current of about 0.7 $\mu A \cdot cm^{-2}$ flowing into the future-emerging point on the primary root.

MATERIALS AND METHODS

Plant Material

The plant used for these experiments was the leguminous plant adzuki (*Phaseolus angularis*). Seeds of adzuki bean were soaked for 4 h in distilled water kept at 40°C and were placed on filter paper moistened with 0.1 mM KCl and 0.05 mM $CaCl_2$ in darkness at 30°C. Six-day-old seedlings with a primary root 100 to 120 mm in length were used.

Measurement System

Figure 1 shows the experimental setup. The electric potential in the solution near the root surface was detected by a computer-controlled microelectrode technique. The electrode had a tip diameter of 200 μm and was filled with 10 mM KCl and 1% agar containing an Ag/AgCl wire. A reference electrode was placed apart from the root. An electric potential pattern was measured precisely and minutely by moving the electrode along the root surface using a newly developed apparatus, which was constructed of an automatic X-Y stage controlled by a computer. The position of the microelectrode relative to the root was observed using a microscope with a video camera attached. The apparatus could resolve separate measuring points with a precision of 10 μm. The electric potentials measured by a digital voltmeter through a high-input impedance amplifier (AD548 [Analog Devices, Tokyo] 3×10^{12} Ω) were stored on a computer.

The root was laid horizontally in a chamber filled with a viscoid aqueous medium (0.1 mM KCl, 0.05 mM $CaCl_2$, and 0.5% methyl cellulose 400), 4 mm in depth, volume 75.3 mL, at 27°C. Methylcellulose 400 was used to make the electrochemical patterns stable; if it was not used, the pattern was disturbed by convection or mechanical vibration. The electrode was moved along the primary root surface at 200-μm intervals while keeping a distance of 200 μm from the surface. The measurement was made in the region along a 6-mm line on the primary root surface in the direction of the longitudinal axis beginning about 70 mm from the root tip. It took about 2 min to measure the electric spatial pattern, and the scannings were made repeatedly over 21 h. The elongation region was about 1 to 5 mm from the tip, and hence this measuring region was the mature region that showed no response to the gravistimulation.

To avoid the influence of the drift of the electrode potential, the electrode was moved adjacent to the reference electrode

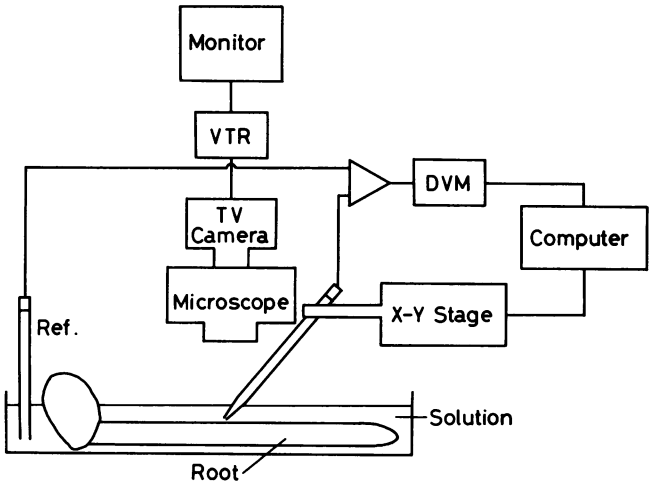

Figure 1. Experimental setup. A root was placed horizontally in a chamber with 0.1 mM KCl + 0.05 mM $CaCl_2$ + 0.5% methyl cellulose 400 solution. The pipet electrode was moved precisely and minutely by a computer-controlled X-Y stage. The electric potentials measured by a digital voltmeter (DVM) were sent to the computer. Changes in the state of the root was recorded through the microscope with the video camera.

and then an offset potential of the electrode was calibrated in each scanning. Figure 2 shows the measured result when this apparatus was used under conditions with only viscoid aqueous medium. A maximum deviation of ±0.1 mV between each scan and a maximum of ±0.07 mV in one scan can be seen during 20 h. This measurement error seems to have originated in the tip potential change of the electrode caused by the movement of the electrode.

THEORY

The one-dimensional electric potential pattern was measured along the surface of a root. Hence, the electric current density in the scanning direction of the electrode is directly estimated from the potential gradient, i.e. the component tangential to the root surface.

The component of electric current density normal to the root surface can be theoretically estimated using the surface electric potential pattern. The validity of the present theory is shown by comparing the calculated electric potential in the two-dimensional plane around a primary root tip with data previously obtained using a multi-electrode measuring apparatus (8).

Basic Equation

In the stationary state, the continuity of the flux of the i-th ionic species is expressed as

$$\nabla \cdot j_i = 0, \tag{1}$$

with the expression for the ionic flux j_i:

$$j_i = -\omega_i RT \nabla c_i - z_i F \omega_i c_i \nabla \phi, \tag{2}$$

where ω_i, z_i, R, T, and F represent the molar mobility, the valency, the gas constant, the absolute temperature, and the Faraday constant, respectively. The ionic flux, the ionic concentration, and the electric potential (denoted by j_i, c_i, and ϕ, respectively) are functions of the space r. The electric current density I in the aqueous medium can be written as

$$I = \sum_i z_i F j_i. \tag{3}$$

Poisson's equation is expressed by

$$\nabla^2 \phi = -\rho/\epsilon, \tag{4}$$

where ϵ represents the dielectric constant of water, and ρ is the electric charge density:

$$\rho = F \sum_i z_i c_i. \tag{5}$$

If we can establish the boundary conditions of the electric potential and the concentrations of all ionic species, the variables $\phi(r)$ and $c_i(r)$ are obtained as the solutions of Equations 1 and 4. However, it is difficult to measure the concentrations of all ionic species at the boundary simultaneously; hence, we try to give an expression for the electric current using two approximations.

The first is electric neutrality, $\rho = 0$, as a common approximation in the aqueous solution. With this approximation, Equation 4 is rewritten to Laplace's equation:

$$\nabla^2 \phi = 0. \tag{6}$$

Using Equation 6 instead of Equation 4, the electric potential distribution can be solved with the measured pattern of the surface electric potential as a boundary condition (see Eq. 10).

The electric current density expressed by Equation 3 depends on the gradients of the electric potential and the ionic concentrations. If the diffusion flux (i.e. the first term on the right side of Eq. 2) and the electrically driven flux (i.e. the second term) are in balance, the flux becomes zero. This represents equilibrium. On the other hand, the roots generate inward and outward fluxes of some specific ions, e.g. H^+, as shown by electric currents (1, 16, 25); hence, the electrically

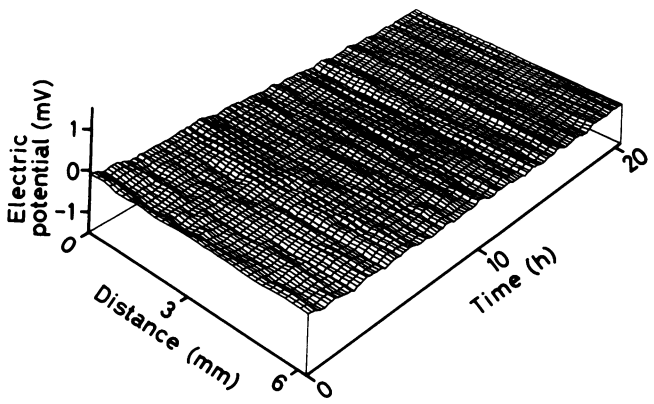

Figure 2. The measurement of electrical potential distribution using the newly developed apparatus where only viscoid aqueous medium was present, without a root.

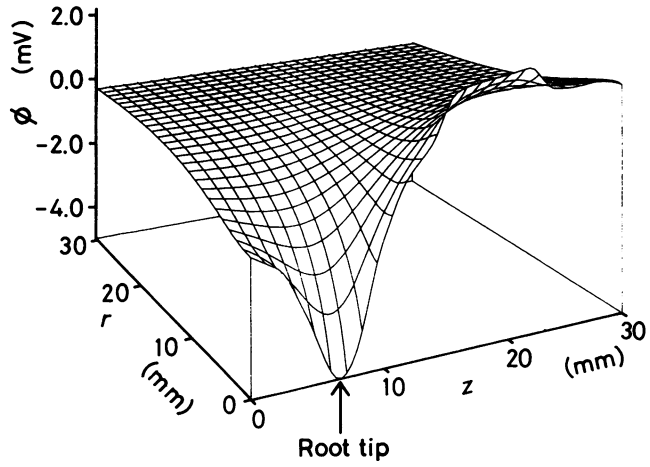

Figure 3. Theoretical result of the electric potential distribution in the two-dimensional plane calculated by Equation 10. The location of the root tip is $z = 6$ mm.

driven flux must be greater than the diffusion flux. As the second approximation, therefore, we put

$$|RT\nabla c_i| \ll |z_i F c_i \nabla \phi|. \quad (7)$$

Under this condition, Equation 3 reduces to

$$I = -\sum_i z_i^2 F^2 \omega_i c_i \nabla \phi. \quad (8)$$

Equation 8 means that the electric potential is connected with the electric current by Ohm's law. The electric current can be approximately calculated by replacing the unknown variable $c_i(r)$ with the average concentration $\bar{c}_i$. This method is similar to the calculation of electric current using the vibrating probe because a specific resistivity of the medium was used (26). Whereas this approximation will lead to an underestimate of electric current due to neglect of diffusion flux, the flow pattern cannot change seriously.

Analysis of Electric Potential Distribution

To confirm the validity using Laplace's equation, Equation 6 was applied to the electric field around a primary root, measured previously using a multi-electrode apparatus (8).

The root was laid horizontally in a thin layer of the medium. Therefore, there was little gradient of the electric potential in a vertical direction except in the region close to the root surface. Thus, the electric potential distribution is calculated in the region of the horizontal plane. The longitudinal and radial coordinates are denoted by z and r, respectively. The measuring region of the surface potential is $0 < z < L_z$ at $r = 0$. The limitation in r direction, L_r, is the location where the electric field is expected to decrease substantially.

The boundary conditions of Equation 6 are established as follows:

$$\phi(0,z) = f(z), \quad (9a)$$

$$\phi(L_r,z) = \int_o^{Lz} f(z)dz, \quad (9b)$$

$$\left.\frac{\partial \phi}{\partial z}\right|_{z = 0,Lz} = 0. \quad (9c)$$

The function $f(z)$ means the measured potential pattern near the root surface ($r = 0$). Equation 9c assumes that there is no electric current flow in the z direction at the two boundaries $z = 0$ and L_z.

Equation 6 with Equations 9a–c can be analytically solved. The solution $\phi(r,z)$ is given by

$$\phi(r,z) = \int_o^{Lz} f(z)\,dz + \sum_{n=1}^{\infty} \frac{2}{L_z} \cos\left(\frac{n\pi z}{L_z}\right) \int_o^{Lz} f(z) \cos\left(\frac{n\pi z}{L_z}\right) dz \cdot \left\{\cosh\left(\frac{n\pi r}{L_z}\right) - \sinh\left(\frac{n\pi r}{L_z}\right) / \tanh\left(\frac{n\pi L_r}{L_z}\right)\right\}. \quad (10)$$

The calculated result of Equation 10 is compared with the experimental data on the two-dimensional measurement of the electric potential around a primary root (8). Figure 3 shows an example of the theoretical potential distribution using Equation 10 under the following conditions: both L_r and L_z are 30 mm, and the measured values at $r = 0$ were adopted as the function $f(z)$ after the interpolation. The electric potential pattern along the root surface decreases monotonicaly with the distance from the surface.

The electric potentials were measured in the region $0 < z < 30$ mm and $0 < r < 10$ mm at 2-mm intervals in each direction. Figure 4 shows comparison of the theoretical values (solid lines) shown in Figure 3 with the experimental values denoted by circles (8). The potential pattern at $r = 6$ mm is shown in Figure 4a and the pattern at $z = 22$ mm, where the largest decrease of potential was observed, is shown in Figure 4b. The estimation errors were as small as 16.4% and 5.2% for Figure 4, a and b, respectively.

The good agreement between the theory and the observed data implies that the above-described theoretical scheme is suitable for the analysis of the electric potential around a root. In the following section, therefore, we calculated the two-dimensional electric current pattern $I(r,z)$ of Equation 8 from the two-dimensional electric potential pattern $\phi(r,z)$, which can be expressed by Equation 10 using the measured one-dimensional electric pattern at the root surface.

RESULTS

Correlation between the Temporal Change in Electric Potential and Growth of Lateral Roots

Figure 5 shows the temporal change in the spatial pattern of one-dimensional electric potential along a root surface. Although a specific pattern of the electric potential was not seen when the measurement started, a valley in the electric potential appeared after a few hours and remained for about 20 h. Figure 6 shows the data extracted from Figure 5 to make clear the change in the pattern of the electric potential. While the electric potential increased as a whole, the pattern hardly changed for the first 30 min. Subsequently, a valley

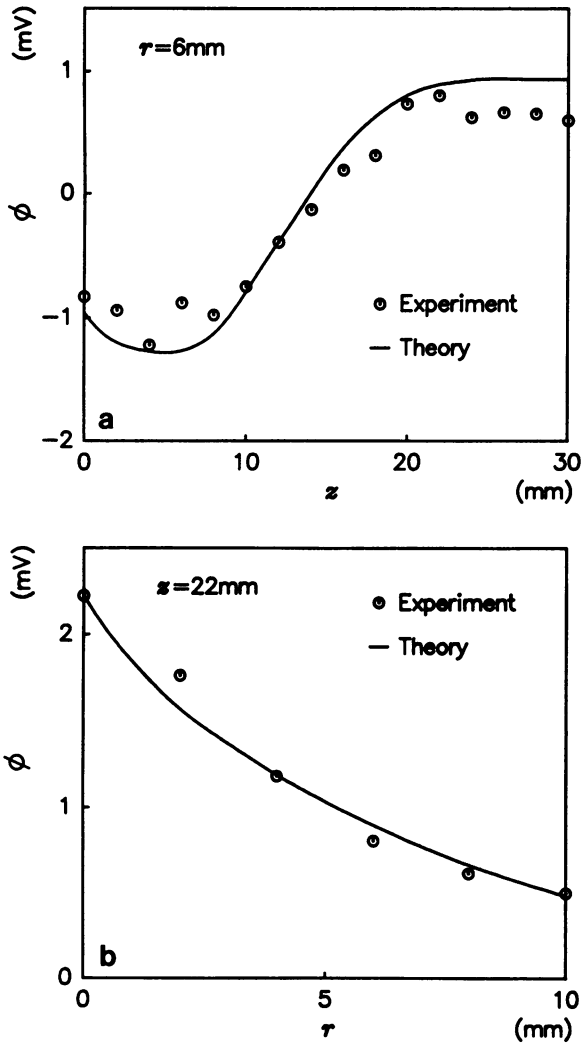

Figure 4. The electric potential distributions in z direction at $r = 6$ mm (a) and r direction at $z = 22$ mm (b). Solid lines are the theoretical values, and circles are experimental data obtained in the previous two-dimensional measurements (8).

in the electric potential appeared around a point 71 mm from the root tip. All of these changes, i.e. the appearance of the potential valley and increment of whole potential, were larger than the measurement error mentioned in Figure 2.

Figure 7 shows pictures of the primary root around the measured region at 0, 4, and 21 h. The calculated two-dimensional patterns of electric current are superimposed based on the theoretical model (Eqs. 8 and 10) mentioned above. Whereas the flow pattern was random at 0 h (a), it became the typical pattern showing influx at the future region of lateral root emergence at 4 h (b). The maximum value of calculated electric current was 0.73 $\mu A \cdot cm^{-2}$ at this stage. It should be noted that a lateral root had not yet emerged by 4 h. A lateral root eventually emerged at the point represented by 71 mm. Electric current flowed into this region at 21 h (c), although current influx had been initiated as early as 4 h (b).

Thirteen examples like Figure 5 have been obtained among 38 roots studied. The valley in electric potential was formed

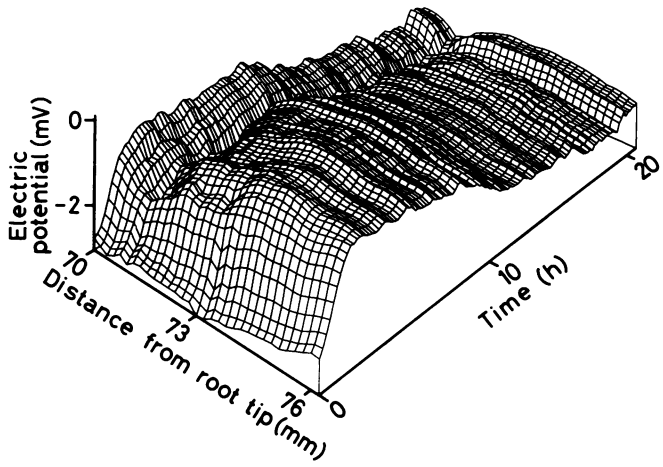

Figure 5. Three-dimensional representation of the spatial pattern of electric potential along a primary root surface over 21 h. The electrode was moved so as to keep a distance of 200 μm from the root surface.

at the point of future lateral root emergence in all cases. The time difference between the appearance of the potential valley and the lateral root emergence was about 5 to 10 h. The depth of the potential valley varied from 1 to 3 mV. In the remaining 25 primary roots, which did not show emergence of lateral roots during measurements, the flow pattern was random (as in Fig. 7a). Because we could not predict the position of lateral root emergence at the start of measurement, we experienced many cases where no lateral roots emerged during the measurement. In some cases, a lateral root emerged on the side of the primary root opposite to where measurements were being made. The electric potential change was not observed in this case, either. This fact implies that the influx occurs locally at the future-emerging point.

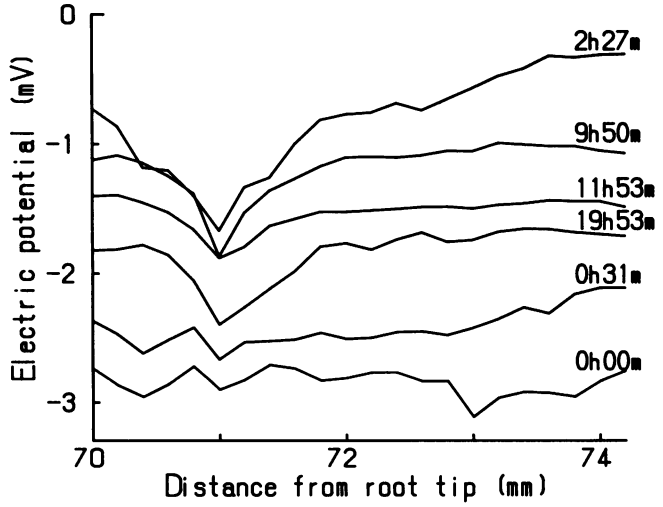

Figure 6. Spatial pattern of electric potential along a root surface. The data were extracted from Figure 5. The label on each curve (0 h 00 m–19 h 53 m) indicates the time from the start of the experiment.

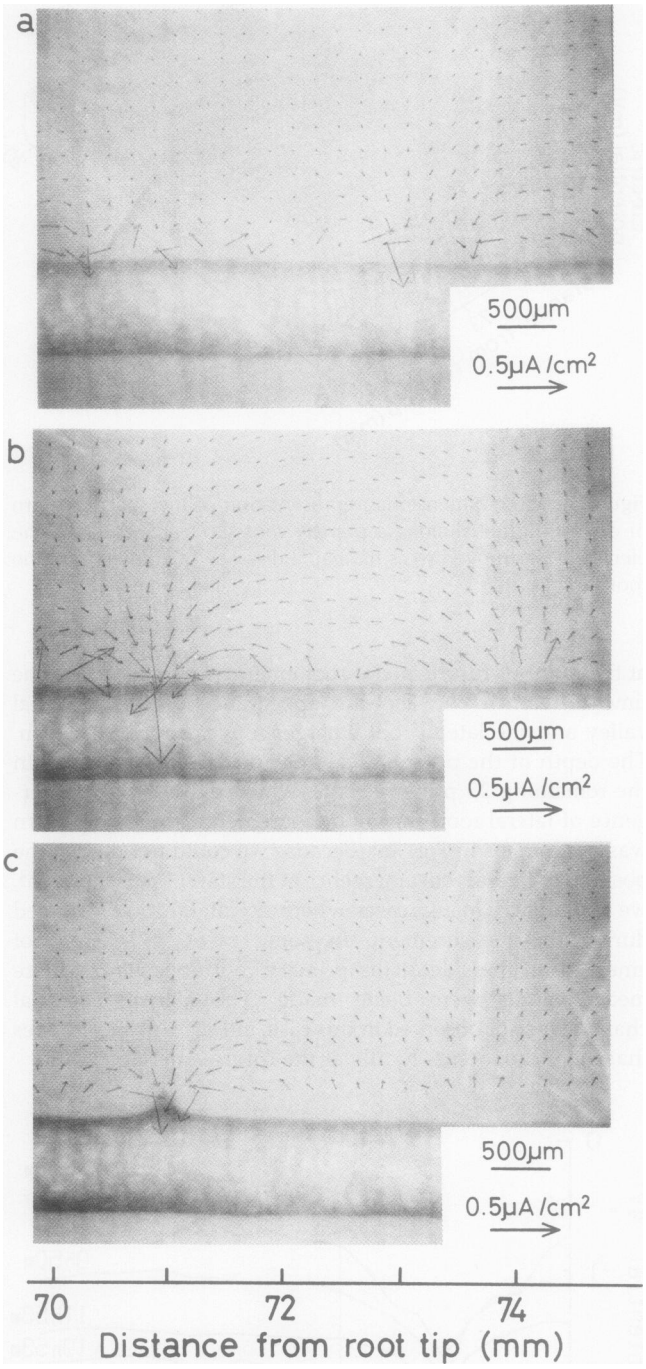

Figure 7. Pictures of the primary root around the measured region at 0 (a), 4 (b), and 21 h (c) from the start of the experiment. The root is the same as in Figure 5. Arrows indicate the electric currents calculated theoretically from the one-dimensional electric potential pattern at the primary root surface. The current density and direction at each location are expressed by the length and direction of the arrow, respectively.

Figure 8 shows the length of the emerged lateral. A lateral root emerged about 12 h after the start of the experiment. As shown in Figure 6, the potential valley appeared more than 10 h before lateral root emergence. In the first 30 min, the potential difference between points of 71 and 72 mm was smaller than 0.2 mV, but later it increased rapidly to 0.8 mV with fluctuations (data not shown). The potential difference fluctuated by about 0.5 mV after the initial increment and also at the emergence of the lateral root.

DISCUSSION

Electric potential (and the electric current density) near the surface of a root can be measured by the microelectrode (11) and the vibrating electrode technique (1, 16, 25, 26). The theory described above can give the two-dimensional electric potential (and electric current) patterns even when only the surface electric potential of a root is measured. The electric current density, as total flux of all ionic species, can be calculated approximately, whereas the flux of respective ionic species in the medium cannot be calculated exactly.

The depth of the potential valley fluctuated (Fig. 5) with an amplitude that was larger than the measurement error; this implies the existence of slow-pulse electric current. Electric or metabolic oscillations can be observed at many stages, e.g. elongation of a primary root (13, 14, 22) and rhizoid formation in *Fucus* (18).

The relation between the electric spatial pattern and growth or morphogenesis has been studied in other organisms. Neurite morphogenetic elongation can be controlled by externally applied current (19). In the brown alga *Fucus*, the appearance of an electric current pattern precedes rhizoid formation (18). Similar current patterns were observed in lateral roots by the vibrating electrode technique (16, 21). Current fluxes of about 0.2 $\mu A \cdot cm^{-2}$ were reported when the primary root surface was deformed by about 50 μm or more as a result of imminent lateral root emergence. This current density is of the same order as the present case (Fig. 7c).

The present result, however, indicates that the current pattern appears as early as 10 h before lateral root emergence.

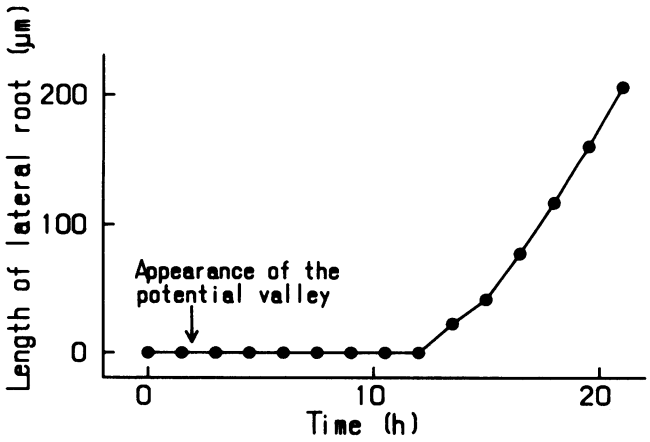

Figure 8. The length of the emerged lateral root. The root is the same as in Figure 5. The valley in the electric potential appeared about 2 h after the start of the experiment.

The electric current flows into the future region of lateral root emergence (Fig. 7b), as in rhizoid formation in *Fucus*. The electric current may carry H^+ to the valley in electric potential, resulting in H^+ accumulation in this region. Generally in plants, acid is known to promote elongation (17), i.e. H^+ loosens a cell wall to cause the elongation. Thus, it would be expected that H^+ helps the lateral root emerge by this mechanism.

On the other hand, primordia of the lateral root are initiated in a region from 3 to 4 cm behind the primary root tip (23, 27). In radish seedlings, the outgrowth (or development) of lateral roots starts inside the primary root about 8 h after primordium formation (3); then the lateral root emerges about 20 h later. Therefore, it is supposed that when the electric potential pattern starts to change (e.g. "2h27m" in Fig. 6), a lateral root primordium starts to grow out inside the primary root. The change in electric potential precedes the emergence of the lateral root. The primary root may generate an influx of electric current into the region where a primordium exists so as to project a lateral root.

The microelectrode technique used here cannot be used with sea water because of its high conductivity; the vibrating electrode is much more powerful in that case. However, the microelectrode technique is effective for studying electric phenomena in lateral-root emergence that occurs in fresh water with low conductivity. There exists the possibility of finding earlier electric events than those found here by using the vibrating electrode. This kind of study may be necessary for more understanding of lateral root emergence or initiation. Furthermore, the two-dimensional measurement at the surface of the primary root may provide new insight.

LITERATURE CITED

1. **Behrens HM, Weisenseel MH, Sievers A** (1982) Rapid changes in the pattern of electric current around the root tip of *Lepidium sativum* L. following gravistimulation. Plant Physiol **70:** 1079–1083
2. **Bisson MA, Walker NA** (1980) The *Chara* plasmalemma at high pH. Electrical measurements show rapid specific passive uniport of H^+ or OH^-. J Membr Biol **56:** 1–7
3. **Blakely LM, Durham M, Evans TA, Blakely RM** (1982) Experimental studies on lateral root formation in radish seedling roots. I. General methods, developmental stages, and spontaneous formation of laterals. Bot Gaz **143:** 341–352
4. **Boels HD, Hansen UP** (1982) Light and electrical current stimulate same feed-back systems in *Nitella*. Plant Cell Physiol **23:** 343–346
5. **Coster HGL, Chilcott TC, Ogata K** (1983) Fluctuations in the electrical properties of *Chara* and the spatial structure of the electrochemical characteristics. *In* WJ Lucas, JA Berry, eds, Inorganic Carbon Uptake by Aquatic Photosynthesis Organisms. Waverly Press, Baltimore, pp 255–269
6. **de Boer AH, Prins HBA, Zanstra PE** (1983) Bi-phasic composition of trans-root electric potential in roots of *Plantago* species: involvement of spatially separated electrogenic pumps. Planta **157:** 259–266
7. **Desrosiers MF, Bandurski RS** (1988) Effect of a longitudinally applied voltage upon the growth of *Zea mays* seedlings. Plant Physiol **87:** 874–877
8. **Ezaki S, Toko K, Yamafuji K** (1990) Electrical stimulation on the growth of a root of the higher plant. Trans In Elec Infor Com Engin **E73:** 922–927
9. **Ezaki S, Toko K, Yamafuji K, Irie F** (1988) Electric potential patterns around a root of the higher plant. Trans In Elec Infor Com Engin **E71:** 965–967
10. **Harold FM, Schreurs WJ, Caldwell JH** (1985) Transcellular ion currents in the water mold *Achlya*. *In* R Nuccitelli, ed, Ionic Currents in Development. Alan R. Liss, New York, pp 89–96
11. **Iiyama S, Toko K, Yamafuji K** (1985) Band structure of surface electric potential in growing roots. Biophys Chem **21:** 285–293
12. **Jaffe LF** (1979) Control of development by ionic currents. *In* RA Cone, JE Dowling, eds, Membrane Transduction Mechanism. Raven Press, New York, pp 199–231
13. **Jenkinson IS, Scott BIH** (1961) Bioelectric oscillations of bean roots: further evidence for a feedback oscillator. Aust J Biol Sci **14:** 231–247
14. **Kristie DN, Jolliffe PA** (1986) High-resolution studies of growth oscillations during stem elongation. Can J Bot **64:** 2399–2405
15. **Lund EJ** (1947) Bioelectric Fields and Growth. University of Texas Press, Austin
16. **Miller AL, Shand E, Gow NAR** (1988) Ion currents associated with root tips, emerging laterals and induced wound sites in *Nicotiana tabacum:* spatial relationship proposed between resulting electrical fields and phytophthoran zoospore infection. Plant Cell Environ **11:** 21–25
17. **Moloney MM, Elliott MC, Cleland RE** (1981) Acid growth effects in maize roots. Evidence for a link between auxin-economy and proton extrusion in the control of root growth. Planta **152:** 285–291
18. **Nuccitelli R, Jaffe LF** (1975) The pulse current pattern generated by developing fucoid eggs. J Cell Biol **64:** 636–643
19. **Patel NB, Poo MM** (1984) Perturbation of the direction of neurite growth by pulsed and local electric fields. J Neurosci **4:** 2939–2947
20. **Pickard BG** (1985) Early events in geotropism of seedling shoots. Annu Rev Plant Physiol **36:** 55–75
21. **Rathore KS, Hotanry KB, Robinson KR** (1990) A two-dimensional vibrating probe study of currents around lateral roots of *Raphanus sativus* developing in culture. Plant Physiol **92:** 543–546
22. **Souda M, Toko K, Hayashi K, Fujiyoshi T, Ezaki S, Yamafuji K** (1990) Relationship between growth and electric oscillations in bean roots. Plant Physiol **93:** 532–536
23. **Street HE** (1966) The physiology of root growth. Annu Rev Plant Physiol **17:** 315–344
24. **Toko K, Iiyama S, Tanaka C, Hayashi K, Yamafuji K, Yamafuji K** (1987) Relation of growth process to spatial patterns of electric potential and enzyme activity in bean roots. Biophys Chem **27:** 39–58
25. **Weisenseel MH** (1983) Control of differentiation and growth by endogenous electric currents. *In* W Hoppe, W Lohmann, H Markl, H Ziegler, eds, Biophysics. Springer-Verlag, Berlin, pp 460–465
26. **Weisenseel MH, Dorn A, Jaffe LF** (1979) Natural H^+ currents traverse growing roots and root hairs of barley (*Hordeum vulgare* L.). Plant Physiol **64:** 512–518
27. **Zeadan SM, Macleod RD** (1984) Apical meristem activity and lateral root anlage development in excised roots of *Pisum sativum* L. Ann Bot **54:** 77–85